

## Ferroelastic Transformations in Lead Orthophosphate and its Structure as a Function of Temperature

BY D. M. C. GUIMARAES\*

Clarendon Laboratory, Parks Road, Oxford OX1 3PU, England

(Received 30 January 1978; accepted 5 July 1978)

### Abstract

In  $\text{Pb}_3(\text{PO}_4)_2$  there are in general triplets of crystallographically independent atoms of the same kind that are pseudosymmetrically related by a pseudo-threefold rotation and interchange identity in ferroelastic transformations. By means of a rotation of axes that takes into account the distortion of the real monoclinic lattice, the atomic coordinates in the ferroelastic transformations of  $\text{Pb}_3(\text{PO}_4)_2$  are calculated. The results of the refinement of the structure by means of the Rietveld technique, at several temperatures below and above the phase transition, are reported, as well as the atomic displacements involved in the ferroelastic switching as a function of temperature.

### 1. Introduction

Ferroelastic  $\text{Pb}_3(\text{PO}_4)_2$  is known to undergo a phase transition at about  $180^\circ\text{C}$ . The space groups and lattice parameters were determined for both phases by Keppler (1970), who also obtained the atomic positions in the low-temperature phase. The phase transition takes place between two phases with space groups  $C2/c$  ( $C_{2h}^6$ , low-temperature,  $\alpha$ , ferroelastic phase) and  $R\bar{3}m$  ( $D_{3d}^5$ , high-temperature,  $\beta$ , prototypic phase). The material belongs to the pure ferroelastic species  $\bar{3}mF2/m$  of Aizu's (1969) classification. The  $\beta$  phase is isomorphous with the structures of barium and strontium orthophosphates (Zachariasen, 1948).

The ferroelastic properties of  $\text{Pb}_3(\text{PO}_4)_2$  were first observed by Brixner, Bierstedt, Jaep & Barkley (1973).

There are, in the  $\alpha$  phase, three possible orientations of the domains (Fig. 1), related to one another by threefold rotation about the reciprocal  $a_m^*$  axis, provided a suitable origin is chosen (pseudo-threefold axis). The subscript  $m$  refers to the monoclinic cell. Thin, transparent crystal plates parallel to the (100) monoclinic plane and perpendicular to the pseudo-threefold axis show, under the polarizing microscope, a pattern of ferroelastic domains, which can easily be trans-

formed to a single domain by applying a small external stress (needle pressure).

The coercive stress was determined by Salje & Hoppmann (1976) and its temperature dependence by von Hodenberg & Salje (1977).

Abrahams & Keve (1971) and Abrahams (1971) examined the properties of ferroelastic crystals in terms of their atomic arrangements, showing that, if two ferroelastic domains are possible, there are within the unit cell pairs of pseudosymmetrically related atoms. Thus, for every atom at  $x_1y_1z_1$ , there is a crystallographically independent atom of the same kind at  $x_2y_2z_2$ , with

$$x_1y_1z_1 = f(x_2y_2z_2) + \Delta, \quad (1)$$

where  $\Delta$  is an atomic displacement of the order of tenths of an ångström and  $f(x_2y_2z_2)$  represents a transformation that contains, in general, translational operators and causes reorientation of the lattice vectors.

In this paper a description of the ferroelastic transformation in  $\text{Pb}_3(\text{PO}_4)_2$  is given. For a crystal, such as lead orthophosphate, which presents three possible kinds of ferroelastic domain, there are in general triplets of crystallographically independent atoms of the same kind that interchange identity when the crystal switches from one orientational state to another, these being pseudosymmetrically related by the pseudo-threefold rotation.

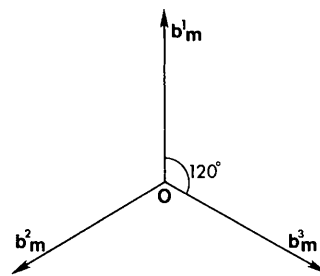


Fig. 1. Three possible orientations of the  $b_m$  axis in ferroelastic  $\text{Pb}_3(\text{PO}_4)_2$ , transforming from a phase of point group  $\bar{3}m$  to a phase of point group  $2/m$ .  $b_m$ ,  $b_m^2$ ,  $b_m^3$  are along the diad axes of symmetry of the former phase.

\* On leave from: Cavendish Laboratory, Madingley Road, Cambridge, England.

Table 1. Interchange identities in the ferroelastic transformations

Domain 1		Domain 2		Domain 3	
Atomic coordinates	Identity of atom	Atomic coordinates	Identity of atom	Atomic coordinates	Identity of atom
$x_1y_1z_1$	O(1)	$r(x_2y_2z_2)$	O(2)	$r'(x_3y_3z_3)$	O(3)
$x_2y_2z_2$	O(2)	$r(x_3y_3z_3)$	O(3)	$r'(x_1y_1z_1)$	O(1)
$x_3y_3z_3$	O(3)	$r(x_1y_1z_1)$	O(1)	$r'(x_2y_2z_2)$	O(2)

## 2. Principle of the method

Ferroelasticity can always be described in terms of a transformation (rotation) of axes, corresponding to the reorientation of the lattice vectors, provided that the distortion of the ferroelastic structure is taken into account. The distortion here is that found in relation to the prototypic phase referred to the axes of the ferroelastic phase.

The calculations carried out with lead orthophosphate exemplify this general method of finding the ferroelastic transformations in ferroelastic materials, when transformation  $f(x_2y_2z_2)$  referred to in (1) cannot be found straightforwardly. The method described below, when applied to simpler ferroelastic transformations, such as in  $\text{SmAlO}_3$ , where the rotation is taken to be through  $90^\circ$ , gives precisely the same results for the atomic displacements as those calculated by Abrahams, Bernstein & Remeika (1974).

Fig. 2 shows a projection of the  $\text{Pb}_3(\text{PO}_4)_2$  ferroelastic structure on the monoclinic (010) plane. The pseudo-threefold axis is along  $a_m^*$  and passes through the point  $(0, \frac{1}{4}, \frac{1}{4})$  with respect to the centre of symmetry.

Consider the  $\text{PO}_4$  tetrahedron marked *T* in Fig. 2. Atoms O(1), O(2) and O(3), which form this tetrahedron with *P* and O(4) almost aligned along the pseudo-threefold axis, are crystallographically independent in the  $\alpha$  phase; they are pseudosymmetrically related by the pseudo-threefold rotation and interchange identity in the ferroelastic transformations as indicated in Table 1.

With atoms *i*, *j* and *k* crystallographically independent atoms of the same kind, we can write

$$x_iy_iz_i = r(x_jy_jz_j) + \Delta \quad (2a)$$

$$x_iy_iz_i = r'(x_ky_kz_k) + \Delta', \quad (2b)$$

where  $i = 1, 2, 3$ ;  $j = 1, 2, 3$ ;  $k = 1, 2, 3$ ;  $i \neq j \neq k$ ;  $r(x_jy_jz_j)$  is a transformation (a rotation of the lattice by  $\theta = 2\pi/3$  about the pseudo-threefold axis) that causes reorientation of the lattice vectors;  $r'(x_ky_kz_k)$  is a similar transformation corresponding to a rotation by  $\theta' = 2 \times 2\pi/3$ ; and  $\Delta$  and  $\Delta'$  are displacement vectors of the order of tenths of an ångström and represent the actual displacements of the atom *i* in the switching process. The ferroelastic transformation concerning the triplet formed by the atoms O(1), O(2) and O(3) results in a small movement of each oxygen atom, e.g. O(1) at  $(x_1y_1z_1)$  goes to the position at  $r(x_2y_2z_2)$ , where it is now O(2) with respect to the transformed lattice, when the crystal switches from domain 1 to domain 2.

An atom which in the  $\beta$  phase lies on the threefold axis, in the  $\alpha$  phase may occur in any one of three possible positions, depending on which domain it is in, which are symmetrically disposed around the pseudo-threefold axis:  $(xyz)$  – domain 1;  $r(xyz)$  – domain 2;  $r'(xyz)$  – domain 3.

In this paper we shall first refer to the transformations on the basis of an ideal threefold symmetry ( $\beta$  phase) and then consider what happens when this is lost ( $\alpha$  phase).

Finally, the results of the refinement of the structure at several temperatures are reported and the atomic displacements necessary for ferroelastic reorientation are calculated.

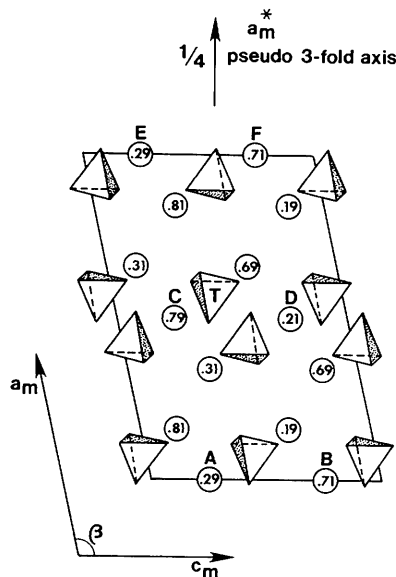


Fig. 2. Projection of the  $\text{Pb}_3(\text{PO}_4)_2$  ferroelastic structure on the (010) monoclinic plane (origin on centre of symmetry). The *y* coordinates are given inside the circles. Pb(1) atoms are labelled as in Fig. 3 [taken from Keppler (1970) but redrawn with minor corrections to the  $\text{PO}_4$  tetrahedra].

### 3. Transformation scheme

#### 3.1. Ideal monoclinic domains in the prototypic phase and ideal transformations

The Pb(1) atoms in the  $\beta$  phase are on  $\bar{3}m$  ( $D_{3d}$ ) sites and define a rhombohedral lattice with three monoclinic sublattices related to one another by the three-fold rotation; the diad axis of each coincides with one of the three diad axes of the parent structure.

In Fig. 3(a) and (b) are shown the relative positions of axes in the rhombohedral lattice (hexagonal axes  $a_r$ ,  $b_r$ ,  $c_r$ ) and monoclinic sublattice ( $a_m, b_m, c_m$ ). This orientation will be called domain 1. The other two sublattices will be similarly referred to as domain 2 and domain 3.

The relationship between the axes is then given by

$$\begin{bmatrix} a_m \\ b_m \\ c_m \end{bmatrix} = \begin{bmatrix} -\frac{2}{3} & -\frac{1}{3} & \frac{2}{3} \\ 0 & -1 & 0 \\ 2 & 1 & 0 \end{bmatrix} \begin{bmatrix} a_t \\ b_t \\ c_t \end{bmatrix} \quad (3)$$

and the axial lengths and  $\cos\beta$  by

$$a_m = \left( \frac{a_t^2}{3} + \frac{4}{9} c_t^2 \right)^{1/2} \quad (4)$$

$$b_m = b_t \quad (5)$$

$$c_m = \sqrt{3} a_t \quad (6)$$

$$\cos\beta = \frac{-a_t\sqrt{3}}{(3a_t^2 + 4c_t^2)^{1/2}} \quad (7)$$

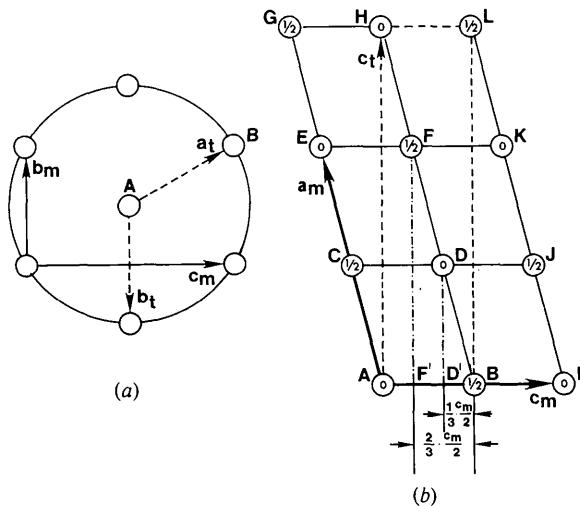


Fig. 3. (a) Disposition of Pb(1) atoms in the  $\beta$  phase on the monoclinic (100) plane, normal to the threefold axis of the rhombohedral cell. (b) Disposition of Pb(1) atoms in the  $\beta$  phase, as seen in projection on the monoclinic (010) plane [origin on Pb(1)]. The  $y$  coordinates are given inside the circles. The projection of the hexagonal cell is shown by dotted lines. [With respect to the centre of symmetry, atom A has coordinates  $(0, \frac{1}{3}, \frac{1}{3})$ .]

In the  $\beta$  phase the following relations between the monoclinic sublattice parameters are obtained:

$$c_m = \sqrt{3}b_m = 3a_m \cos(\pi - \beta). \quad (8)$$

The  $3 \times 3$  matrices that give the transformations between atomic positions in different domains in the  $\beta$  phase can be found by studying the relationships between the monoclinic sublattice axes for those domains.

If the three domains are considered to be related by threefold rotation in an anticlockwise sense, the axes for the transformation of coordinates must correspondingly be rotated in a clockwise sense.

Fig. 3 shows the monoclinic sublattice axes in domain 1. As the arrangement of Pb(1) atoms forms a rhombohedral cell, the axes for the transformation of coordinates in domain 2 and domain 3 are easily found, and related to the axes in domain 1. Axes and coordinates in the three domains ( $\beta$  and  $\alpha$  phases) are denoted by superscripts 1, 2, and 3. [ $a_m^2$  is defined by  $\overline{AF}$  and  $a_m^3$  by  $\overline{AF''}$ ,  $F''$  being a Pb(1) atom directly below  $F$ ; the monoclinic (100) plane is common to the three domains, even in the  $\alpha$  phase, and so the  $b_m^2, c_m^2, b_m^3, c_m^3$  axes are determined straightforwardly.]

It is therefore possible to express the coordinates of an atom in domain 2 and domain 3 in terms of a rotation applied to an appropriate atom in domain 1.

#### 3.2. Real monoclinic lattice and ferroelastic transformations

The real ferroelastic monoclinic lattice is slightly distorted in relation to the ideal monoclinic sublattice of the rhombohedral  $\beta$  phase. A comparison of  $\alpha$  and  $\beta$  structures was given by Keppler (1970) and by Joffrin, Benoit, Deschamps & Lambert (1977). The rhombohedral  $c_r$  axis becomes a pseudo-threefold axis (Figs. 2 and 3); but in the  $\alpha$  phase no atom lies exactly on the pseudo-threefold axis, although Pb(1), Pb(2), P and O(4) are close to it. In the  $\beta$  phase these atoms lie exactly on the threefold axis. This means that their  $y$  coordinate is  $\frac{1}{4}$  and their  $z$  coordinate is such that

$$z = \frac{1}{4} - \frac{a_m}{c_m} x \cos\beta = \frac{1}{4} + \frac{x}{3}$$

(origin at the centre of symmetry). This relation is not exactly true in the  $\alpha$  phase.

Here, the relation  $c_m/b_m$  becomes less than  $\sqrt{3}$ , e.g. at room temperature  $c_m/b_m = 1.655$ . Also, atoms  $D$  and  $F$  (Fig. 3) do not project on to (100) at distances exactly equal to  $c_m/2 \times \frac{1}{3}$  and  $c_m/2 \times \frac{2}{3}$ , respectively, from atom  $B$  along  $c_m$ , as in the  $\beta$  phase. At room temperature the fractional distance  $D'B$  along  $c_m$  is given by

$$D'B = -\frac{1}{2} \frac{a_m}{c_m} \cos\beta = 0.156$$

instead of  $\frac{1}{6}$ .

In Fig. 4(a) the nature of the distortion of the pseudo-hexagonal arrangement of Pb(1) atoms in the (100) plane is shown. The points marked by full circles represent the positions that the Pb(1) atoms would occupy if the only effects were to compress along  $c_m$  and expand along  $b_m$ . However, the actual distortion is more complicated than this, as denoted by the open circles. External stress may cause the atoms to be displaced cooperatively, giving another orientation to the lattice. Fig. 4(b) shows schematically the effective rotation of the hexagonal distortion of the arrangement of Pb(1) atoms.

In order to obtain coordinates in domains 2 and 3, we use rotations of the lattice by  $2\pi/3$  and  $2 \times 2\pi/3$ , respectively, about the reciprocal  $a_m^*$  axis, common to the three domains (pseudo-threefold axis). As in the previous section the domains are considered to be disposed around  $a_m^*$  in an anticlockwise sense, and the rotations of the axes in the transformations are therefore taken in a clockwise sense.

To find the matrices for the real ferroelastic transformations it is simpler to transform first to a set of orthogonal axes  $a_o^1, b_o^1, c_o^1$ , such that  $b_o^1$  and  $c_o^1$  coincide respectively with  $b_m^1$  and  $c_m^1$ , and  $a_o^1$  perpendicular to both, coincides with  $a_m^*$ . [Note that the origin is  $(0, \frac{1}{4}, \frac{1}{4})$  in relation to the centre of symmetry.]

Using matrix notation, we may write

$$\begin{bmatrix} x^1 \\ y^1 \\ z^1 \end{bmatrix} = X^1, \quad \begin{bmatrix} x_o^1 \\ y_o^1 \\ z_o^1 \end{bmatrix} = X_o^1, \quad \text{etc.},$$

so that

$$X_o^1 = HX^1,$$

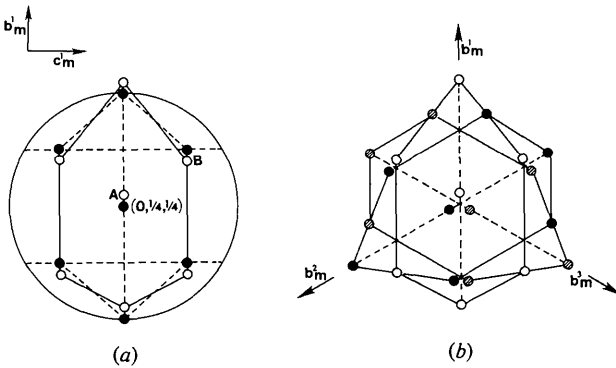


Fig. 4. (a) Schematic representation of the pseudo-hexagonal arrangement of Pb(1) atoms in the  $\alpha$  phase on the monoclinic (100) plane.  $c_m/b_m$  is less than  $\sqrt{3}$ . Open circles: Pb(1) atoms. Closed circles: points at  $(0, \frac{1}{4}, \frac{1}{4})$ ,  $(0, \frac{3}{4}, \frac{3}{4})$ , etc. (b) Rotation of the distortion by means of external stress [monoclinic (100) plane]. Open circles: Pb(1) atoms in domain 1. Closed circles: Pb(1) atoms in domain 2. Hatched circles: Pb(1) atoms in domain 3.

where

$$H = \begin{bmatrix} \sin \beta & 0 & 0 \\ 0 & 1 & 0 \\ \frac{a_m}{c_m} \cos \beta & 0 & 1 \end{bmatrix}. \quad (9)$$

A rotation of the lattice by  $2\pi/3$  about  $a_m^*$  gives the fractional orthogonal coordinates in domain 2:

$$X_o^2 = RX_o^1 = RHX^1; \quad (10)$$

R has the form

$$R = \begin{bmatrix} 1 & 0 & 0 \\ 0 & -\frac{1}{2} & \frac{\sqrt{3}}{2} \cdot u \\ 0 & -\frac{\sqrt{3}}{2} \cdot \frac{1}{u} & -\frac{1}{2} \end{bmatrix}, \quad (11)$$

where  $u = c_m/b_m$ .

To obtain the coordinates in domain 2 referred to the original axes of domain 1, the matrix transformation will be

$$X^2 = H^{-1}X_o^2 = H^{-1}RHX^1 \quad (12)$$

where  $H^{-1}$  is the inverse of matrix H.

The result is

$$\begin{bmatrix} x^2 \\ y^2 \\ z^2 \end{bmatrix} = \begin{bmatrix} 1 & 0 & 0 \\ \frac{\sqrt{3}}{2} u \frac{a_m}{c_m} \cos \beta & -\frac{1}{2} & \frac{\sqrt{3}}{2} u \\ -\frac{3}{2} \frac{a_m}{c_m} \cos \beta & -\frac{\sqrt{3}}{2} \cdot \frac{1}{u} & -\frac{1}{2} \end{bmatrix} \begin{bmatrix} x^1 \\ y^1 \\ z^1 \end{bmatrix}. \quad (13)$$

For domain 3, we find

$$X^3 = H^{-1}R'HX^1 \quad (14)$$

where

$$R' = \begin{bmatrix} 1 & 0 & 0 \\ 0 & -\frac{1}{2} & -\frac{\sqrt{3}}{2} u \\ 0 & \frac{\sqrt{3}}{2} \cdot \frac{1}{u} & -\frac{1}{2} \end{bmatrix}. \quad (15)$$

Therefore

$$\begin{bmatrix} x^3 \\ y^3 \\ z^3 \end{bmatrix} = \begin{bmatrix} 1 & 0 & 0 \\ -\frac{\sqrt{3}}{2} u \frac{a_m}{c_m} \cos \beta & -\frac{1}{2} & -\frac{\sqrt{3}}{2} u \\ -\frac{3}{2} \frac{a_m}{c_m} \cos \beta & \frac{\sqrt{3}}{2} \cdot \frac{1}{u} & -\frac{1}{2} \end{bmatrix} \begin{bmatrix} x^1 \\ y^1 \\ z^1 \end{bmatrix}. \quad (16)$$

In the high-temperature phase, owing to relations (8), the element  $(a_m/c_m) \cos \beta$  in matrix (9) is equal to  $-\frac{1}{3}$  and the quantity  $u$  in matrices (11) and (15) is equal to  $\sqrt{3}$ ; matrices (9), (11) and (15) therefore take into account the distortion present when the structure is in its low-temperature modification. Matrices (13) and (16) give the transformed coordinates in domains 2 and 3, axes of reference being those chosen for domain 1.

Thus, for example, if we refer to relations (2) and Table 1, equation (13) relates O(1) in domain 1, with coordinates  $(x_1, y_1, z_1)$  to O(1) in domain 2, with coordinates  $r(x_1, y_1, z_1)$ . Note that although we are relating two atomic positions by a rotation, we emphasize that the *actual* movement of the atoms in question is only a small displacement. For example, O(1) in domain 2 is actually produced during the ferroelastic switching by a small displacement  $\Delta$  of O(3) in domain 1 [ $x_3, y_3, z_3 = r(x_1, y_1, z_1) + \Delta$ ], where  $\Delta = 0.16 \text{ \AA}$ .

#### 4. Neutron diffraction; results and discussion

Neutron diffraction measurements were carried out on the powder diffractometer PANDA at AERE (Harwell) at several temperatures: 25, 70, 150, 160, 170, 200, 250 and 350°C ( $\pm 5^\circ\text{C}$ ). The sample was contained in a 16 mm diameter thin-walled vanadium can and the neutron wavelength was about 1.32 Å. The diffracted intensities were measured by a bank of nine BF<sub>3</sub> counters. The counter bank swept through  $5^\circ < 2\theta < 110^\circ$  in steps of  $0.10^\circ$ . The measurements were made over a period of about 24 h. The counts were merged together with a set of specially designed computer programs.

The structure, at different temperatures, was refined by the neutron-powder profile technique (Rietveld, 1969; Hewat, 1973).

Above the transition temperature  $T_0$  the refinement of the structure was carried out using hexagonal axes (space group  $R\bar{3}m$ ) and the results are shown in Table 2.

The O(2) atoms referred to in Table 2 are symmetry-related, having hexagonal coordinates  $(x, \bar{x}, z)$ ,  $(x, 2x, z)$ ,  $(2\bar{x}, \bar{x}, z)$ . For comparison with the ferroelastic phase, their monoclinic coordinates are written in Table 3 as belonging to independent atoms O(1), O(2), O(3); the O(1) atom in Table 2 becomes O(4) in Table 3.

Table 3 lists monoclinic lattice parameters and atomic coordinates at all temperatures given by the refinements below and above the phase transition. Above  $T_0$  the monoclinic lattice parameters and coordinates are calculated from the hexagonal ones by equations (3) to (7).

Fig. 5 shows the experimental and calculated profiles for Pb<sub>3</sub>(PO<sub>4</sub>)<sub>2</sub> at room temperature and at 250°C.

Table 2. Lattice and positional parameters of Pb<sub>3</sub>(PO<sub>4</sub>)<sub>2</sub> at 200, 250 and 350°C (hexagonal axes)

Standard deviations are given in parentheses.

Temperature (°C)	200	250	350
Space group	$R\bar{3}m$	$R\bar{3}m$	$R\bar{3}m$
Lattice parameters			
$a_i$ (Å)	5.530 (2)	5.549 (1)	5.548 (1)
$c_i$ (Å)	20.277 (3)	20.345 (3)	20.362 (3)
Pb(1)			
$x_i$	0	0	0
$y_i$	0	0	0
$z_i$	0	0	0
Pb(2)			
$x_i$	0	0	0
$y_i$	0	0	0
$z_i$	0.214 (1)	0.212 (1)	0.213 (1)
P			
$x_i$	0	0	0
$y_i$	0	0	0
$z_i$	0.402 (1)	0.402 (1)	0.403 (1)
O(1)			
$x_i$	0	0	0
$y_i$	0	0	0
$z_i$	0.327 (1)	0.328 (1)	0.328 (1)
O(2)			
$x_i$	-0.151 (1)	-0.151 (1)	-0.150 (1)
$y_i$	0.151 (1)	0.151 (1)	0.150 (1)
$z_i$	0.427 (1)	0.428 (1)	0.429 (1)

Table 4 shows the variation of the displacement vectors [defined by (2)] with temperature in the  $\alpha$  phase. These displacements are of course zero in the  $\beta$  phase.

It can be seen from Tables 3 and 4 that the distortion of the  $\alpha$  phase diminishes progressively as the

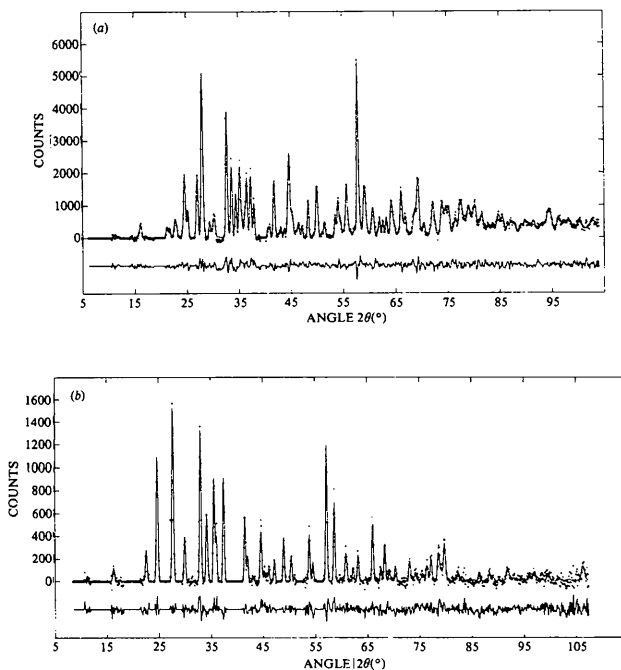


Fig. 5. Powder neutron diffraction profiles for Pb<sub>3</sub>(PO<sub>4</sub>)<sub>2</sub> (a) at room temperature and (b) at 250°C, showing observed (crosses) and calculated (solid line) profiles. The bottom trace is the difference profile.

Table 3. *Lattice and positional parameters of Pb<sub>3</sub>(PO<sub>4</sub>)<sub>2</sub> at several temperatures below and above T<sub>0</sub> (monoclinic axes)*

The origin is at the centre of symmetry. Standard deviations are given in parentheses.

Temperature (°C)	Room temperature	70	150	160	170	200	250	350
Space group	C2/c	C2/c	C2/c	C2/c	F2/m	R3m	R3m	R3m
Lattice parameters								
<i>a</i> (Å)	13.80 (1)	13.83 (1)	13.86 (1)	13.91 (2)	13.91 (2)	13.89 (1)	13.94 (1)	13.95 (1)
<i>b</i> (Å)	5.691 (1)	5.655 (1)	5.589 (1)	5.555 (2)	5.553 (2)	5.530 (2)	5.549 (1)	5.548 (1)
<i>c</i> (Å)	9.42 (1)	9.46 (1)	9.53 (1)	9.59 (2)	9.59 (2)	9.58 (1)	9.61 (1)	9.61 (1)
$\beta$ (°)	102.3 (1)	102.6 (1)	102.9 (1)	103.1 (1)	103.1 (1)	103.3 (1)	103.3 (1)	103.3 (1)
Pb(1)	<i>x</i>	0	0	0	0	0	0	0
	<i>y</i>	0.291 (2)	0.281 (3)	0.276 (2)	0.275 (5)	$\frac{1}{4}$	$\frac{1}{4}$	$\frac{1}{4}$
	<i>z</i>	$\frac{1}{4}$	$\frac{1}{4}$	$\frac{1}{4}$	$\frac{1}{4}$	$\frac{1}{4}$	$\frac{1}{4}$	$\frac{1}{4}$
Pb(2)	<i>x</i>	0.317 (1)	0.320 (1)	0.321 (1)	0.321 (1)	0.321 (1)	0.319 (1)	0.320 (1)
	<i>y</i>	0.309 (1)	0.305 (1)	0.292 (2)	0.273 (4)	$\frac{1}{4}$	$\frac{1}{4}$	$\frac{1}{4}$
	<i>z</i>	0.352 (1)	0.354 (1)	0.356 (1)	0.352 (3)	0.349 (2)	0.357 (1)	0.357 (1)
P	<i>x</i>	0.599 (1)	0.603 (1)	0.606 (1)	0.604 (1)	0.605 (1)	0.603 (1)	0.602 (1)
	<i>y</i>	0.241 (2)	0.247 (4)	0.240 (3)	0.242 (5)	$\frac{1}{4}$	$\frac{1}{4}$	$\frac{1}{4}$
	<i>z</i>	0.447 (1)	0.447 (2)	0.448 (2)	0.443 (3)	0.448 (3)	0.451 (1)	0.451 (1)
O(1)	<i>x</i>	0.643 (1)	0.647 (1)	0.651 (1)	0.650 (2)	0.645 (1)	0.641 (1)	0.643 (1)
	<i>y</i>	0.030 (1)	0.033 (3)	0.026 (3)	0.030 (5)	0.032 (3)	0.023 (1)	0.024 (1)
	<i>z</i>	0.392 (1)	0.386 (2)	0.389 (2)	0.392 (3)	0.383 (2)	0.388 (1)	0.389 (1)
O(2)	<i>x</i>	0.634 (1)	0.636 (1)	0.637 (1)	0.639 (2)	0.645 (1)	0.641 (1)	0.643 (1)
	<i>y</i>	0.464 (1)	0.469 (3)	0.469 (3)	0.477 (5)	0.468 (3)	0.477 (1)	0.476 (1)
	<i>z</i>	0.374 (1)	0.381 (2)	0.385 (2)	0.382 (3)	0.383 (2)	0.388 (1)	0.389 (1)
O(3)	<i>x</i>	0.642 (1)	0.642 (1)	0.643 (1)	0.637 (2)	0.635 (2)	0.641 (1)	0.643 (1)
	<i>y</i>	0.280 (2)	0.278 (2)	0.270 (2)	0.271 (5)	$\frac{1}{4}$	$\frac{1}{4}$	$\frac{1}{4}$
	<i>z</i>	0.612 (1)	0.617 (1)	0.618 (1)	0.621 (3)	0.620 (3)	0.615 (1)	0.615 (1)
O(4)	<i>x</i>	0.491 (1)	0.490 (1)	0.489 (1)	0.492 (1)	0.490 (1)	0.491 (1)	0.493 (1)
	<i>y</i>	0.222 (2)	0.228 (3)	0.230 (3)	0.246 (5)	$\frac{1}{4}$	$\frac{1}{4}$	$\frac{1}{4}$
	<i>z</i>	0.420 (1)	0.416 (2)	0.414 (2)	0.412 (3)	0.421 (3)	0.414 (1)	0.414 (1)

Table 4. *Displacement vectors in the ferroelastic phase at several temperatures*

$\Delta$ ,  $\Delta'$ , and  $\Delta''$  correspond respectively to the switching (1  $\rightarrow$  2), (1  $\rightarrow$  3), (2  $\rightarrow$  3) and are given in ångströms. 1, 2, 3 refer to the three ferroelastic domains as in the text. Only one value is given when it is the same for  $\Delta$ ,  $\Delta'$ , and  $\Delta''$ . Standard deviations are given in parentheses.

Temperature (°C)	25	70	150	160	170	
Space group	C2/c	C2/c	C2/c	C2/c	F2/m	
Pb(1)	$\Delta$	0.41 (1)	0.31 (2)	0.25 (2)	0.24 (3)	0
	$\Delta'$					
	$\Delta''$					
Pb(2)	$\Delta$	0.58 (1)	0.54 (1)	0.41 (1)	0.22 (3)	0.12 (3)
	$\Delta'$					
	$\Delta''$					
P	$\Delta$	0.17 (1)	0.09 (2)	0.10 (2)	0.12 (4)	0.03 (2)
	$\Delta'$					
	$\Delta''$					
O(1)	$\Delta$	0.19 (1)	0.16 (2)	0.20 (2)	0.17 (4)	0.11 (3)
	$\Delta'$	0.16 (1)	0.20 (2)	0.16 (2)	0.25 (4)	0.18 (3)
	$\Delta''$	0.23 (1)	0.25 (2)	0.19 (2)	0.12 (4)	0.18 (3)
O(2)	$\Delta$	0.23 (1)	0.25 (2)	0.19 (2)	0.12 (4)	0.18 (3)
	$\Delta'$	0.19 (1)	0.16 (2)	0.20 (2)	0.17 (4)	0.11 (3)
	$\Delta''$	0.16 (1)	0.20 (2)	0.16 (2)	0.25 (4)	0.18 (3)
O(3)	$\Delta$	0.16 (1)	0.20 (2)	0.16 (2)	0.25 (4)	0.18 (3)
	$\Delta'$	0.23 (1)	0.25 (2)	0.19 (2)	0.12 (4)	0.18 (3)
	$\Delta''$	0.19 (1)	0.16 (2)	0.20 (2)	0.17 (4)	0.11 (3)
O(4)	$\Delta$	0.38 (1)	0.27 (2)	0.21 (2)	0.04 (4)	0.15 (3)
	$\Delta'$					
	$\Delta''$					

Table 5. *R* factors (nuclear) (%) at all temperatures for the three space groups

	Room temperature	70°C	150°C	160°C	170°C	200°C	250°C	350°C
<i>C2/c</i>	5.87	8.11	6.75	10.57	10.57	—	—	—
<i>F2/m</i>	14.76	15.22	10.58	10.62	9.34	—	—	—
<i>R3̄m</i>	—	—	—	—	—	11.91	10.72	8.39

transition is approached from below and the structural parameters approach the values corresponding to the  $\beta$  phase.

The space group assumed for the  $\alpha$  phase was *C2/c* at room temperature, 70, 150 and 160°C. At 170°C poor results were obtained in the refinement unless the space group was taken to be *F2/m* (Ng & Calvo, 1975), in which case a mirror plane appears at  $y = \frac{1}{4}$ , the cell becoming face-centred before the threefold axis develops. At 160°C, the application of significance tests (Hamilton, 1965) suggests rejection of space group *F2/m* at the 0.5% significance level.

Below the phase transition the refinements were also repeated in all cases assuming the space group *F2/m*. Despite large errors, the results shown in Table 5 agree with the conclusion that, although the space group *F2/m* probably does not actually exist (Joffrin *et al.*, 1977), the constraints imposed on the atomic coordinates allow better refinement when the structure is so close to the high-symmetry phase. Attempts at refining the 170°C data in *R3̄m* failed, as did refinement of the 200°C data in *F2/m*.

Table 5 also shows that in the  $\beta$  phase the final *R* factors decrease as the temperature is raised above  $T_0$ , a result compatible with the hypothesis that monoclinic microdomains exist in the high-temperature phase but vanish progressively as the temperature is raised (Joffrin *et al.*, 1977). Moreover, in the  $\alpha$  phase, there is an improvement in all the refinements if anisotropic temperature factors for all the atoms are assumed (although they probably have no real meaning). In the  $\beta$  phase, at 200°C, a significant improvement is obtained using anisotropic temperature factors for all atoms; however, at 250 and 350°C, this is not so, and the refinements were carried out, therefore, with isotropic temperature factors for all atoms.

The displacement vectors for O(1), O(2) and O(3) (Table 4) do not show much temperature dependence, except that the PO<sub>4</sub> tetrahedron undergoes an abrupt movement at the transition temperature, when the plane defined by O(1), O(2), O(3) becomes perpendicular to  $a_m^*$  and the P—O(4) bond is aligned with this axis. This result is compatible with a first-order transition. The value of  $\Delta$  for O(4) at 170°C is probably anomalously large as a result of the use of space group *F2/m*.

The relatively high values found for the atomic displacements  $\Delta$  at room temperature [particularly for Pb(2), Pb(1) and O(4) — almost 0.6 Å for Pb(2)] agrees with the large room-temperature value of the spontaneous strain, one of the largest that is known (Toledano, Pateau, Primot, Aubrée & Morin, 1975). It is interesting to note that the atoms with the largest values of  $\Delta$  are those closest to the pseudo-threefold axis (with the exception of P). They also seem to be the most temperature dependent and therefore are probably the major contributors to the ferroelastic properties of this material.

The author acknowledges with gratitude the advice and assistance of Dr A. M. Glazer who critically read the manuscript and made useful suggestions, and thanks the Clarendon Laboratory, Oxford, for providing facilities.

A grant from the Portuguese Government (INIC) is also acknowledged.

#### References

- ABRAHAMS, S. C. (1971). *Mater. Res. Bull.* **6**, 881–890.  
 ABRAHAMS, S. C., BERNSTEIN, J. L. & REMEIK, J. P. (1974). *Mater. Res. Bull.* **9**, 1613–1616.  
 ABRAHAMS, S. C. & KEVE, E. T. (1971). *Ferroelectrics*, **2**, 129–154.  
 AIZU, K. (1969). *J. Phys. Soc. Jpn*, **27**, 387–396.  
 BRIXNER, L. H., BIERSTEDT, P. E., JAEP, W. F. & BARKLEY, J. R. (1973). *Mater. Res. Bull.* **8**, 497–504.  
 HAMILTON, W. C. (1965). *Acta Cryst.* **18**, 502–510.  
 HEWAT, A. W. (1973). *J. Phys. C*, **6**, 2559–2572.  
 HODENBERG, R. VON & SALJE, E. (1977). *Mater. Res. Bull.* **12**, 1029–1034.  
 JOFFRIN, C., BENOIT, J. P., DESCHAMPS, L. & LAMBERT, M. (1977). *J. Phys. (Paris)*, **38**, 205–213.  
 KEPPLER, U. (1970). *Z. Kristallogr.* **132**, 228–235.  
 NG, H. N. & CALVO, C. (1975). *Can. J. Phys.* **53**, 42–51.  
 RIETVELD, H. M. (1969). *J. Appl. Cryst.* **2**, 65–71.  
 SALJE, E. & HOPPMANN, G. (1976). *Mater. Res. Bull.* **11**, 1545–1549.  
 TOLEDANO, J. C., PATEAU, L., PRIMOT, J., AUBRÉE, J. & MORIN, D. (1975). *Mater. Res. Bull.* **10**, 103–112.  
 ZACHARIASEN, W. H. (1948). *Acta Cryst.* **1**, 263–265.